# Relation of Structural Changes to Electron-Transfer Parameters in Fulvalenediyl Dirhodium Complexes Demonstrating Quasi-Reversible Two-Electron Voltammetry†

**Teen T. Chin,‡ William E. Geiger,*,‡ and Arnold L. Rheingold§**

*Contribution from the Departments of Chemistry, University of Vermont, Burlington, Vermont 05405, and University of Delaware, Newark, Delaware 19716*

*Received January 24, 1996*⊗

**Abstract:** The oxidations of two fulvalenediyl (Fv) dirhodium complexes [(Fv)$Rh_2(CO)_4$, **1**, and (Fv)$Rh_2(CO)_2$($\mu$-dppm), **2**] have been studied by voltammetry, coulometry, IR spectroelectrochemistry, UV−VIS spectroscopy, and X-ray crystallography. Both complexes undergo net two-electron oxidations to dications having a Rh−Rh bond. The M−M bond distances are 2.837(1) Å in $\mathbf{2}^{2+}$ and 4.511(1) Å in **2**. Quasi-reversible cyclic voltammetric responses were exploited over a range of sweep rates to give CV curves successfully fit to an EE mechanism by digital simulations: for **1**, $E^{\circ\prime}_1 = -0.10$ V (*vs* Fc), $k_{s1} = 0.013$ cm $s^{-1}$, $(1 - \alpha_1) = 0.66$, $E^{\circ\prime}_2 = -0.24_5$ V, $k_{s2} = 0.044$ cm $s^{-1}$, $\alpha_2 = 0.5$; for **2**, $E^{\circ\prime}_1 = -0.76$ V, $k_{s1} = 0.035$ V, $(1 - \alpha_1) = 0.75$, $E^{\circ\prime}_2 = -0.77_6$ V, $k_{s2} > 0.2$ cm $s^{-1}$, $\alpha_2 = 0.5$. Complementary results were obtained for the reduction of the dications $\mathbf{1}^{2+}$ or $\mathbf{2}^{2+}$. The effect of the bridging fulvalenediyl ligand is to retard the oxidation process by an amount consistent with the calculated barrier to rotation around the C−C bond of the $\eta^5,\eta^{5\prime}$-$C_{10}H_8$ ligand. In both complexes the 0/1+ redox process is slower than the 1+/2+ process. The electron transfer rates are consistent with a progressive increase in the Rh−Rh bond order in the 0/1+/2+ charged complexes rather than full M−M bond formation and cleavage in a single step.

## Introduction

This paper compares the electron-transfer characteristics of two fulvalenediyl[1] (Fv) complexes which undergo making and breaking of a metal−metal bond during two-electron reactions requiring different geometric pathways. Both (Fv)$Rh_2(CO)_4$, **1**, and (Fv)$Rh_2(CO)_2$(dppm),[2] **2**, oxidize in single two-electron voltammetric waves to dications having Rh−Rh bonds, in spite of the fact that the disposition of the metals in *anti* in **1** and *syn* in **2**.

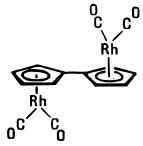


**1**

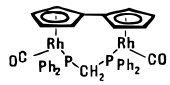


**2**

It has been observed that two-electron transfers (defined here as those involving a thermodynamically-disfavored one-electron intermediate) may provide low-energy pathways to structural changes coupled to the redox process.[3−15] Schultz has pointed out that the activation energy required for *sequential* transfer of two electrons at the same potential (eq 1) is only one-fourth of that required for a *concerted* two-electron process (eq 2) because $\Delta G^{\ddagger}$ varies with the square of the atomic displacements, $\Delta a_i^2$ (eq 3).[9]

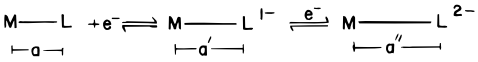


(1)

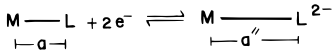


(2)

$$\Delta G^{\ddagger} \propto \Delta a_i^2 \tag{3}$$

Hence, large molecular displacements may be potentially achieved with retention of rapid electron-transfer kinetics if the displacements are coupled to an EE electron-transfer mechanism. A consequence of this hypothesis is that compounds displaying two-electron CV waves of near-Nernstian character may still experience large geometric changes in the overall reaction.

The mechanisms of multielectron transfer reactions are being increasingly investigated to learn more about the factors that

† Structural Consequences of Electron-Transfer Reactions. 32. For parts 30 and 31, see: *Acc. Chem. Res.* **1995**, *28*, 351 and *J. Am. Chem. Soc.* **1995**, *117*, 12202. The term "quasi-reversible" is used in the context of charge-transfer properties in the kinetic regime originally outlined by Matsuda (see ref 45, pp 224 ff).

‡ University of Vermont.

§ University of Delaware.

⊗ Abstract published in *Advance ACS Abstracts,* May 1, 1996.

(1) The $[\eta^5,\eta^{5\prime}$-$C_{10}H_8]^{2-}$ ligand is referred to as fulvalenediyl rather than as the more commonly-used fulvalene to emphasize its analogy to the $[\eta^5$-$C_5H_5]^-$ (cyclopentadienyl) ligand.

(2) Abbreviations used in this paper: $\alpha$ = charge transfer coefficient, CV = cyclic voltammetry, dppm = diphenylphosphinomethane, $\delta = E_p - E_{p/2}$, $\Delta E_p = E_{pa} - E_{pc}$, et = electron transfer, Fv = fulvalenediyl, OTTLE = optically transparent thin layer electrode, $\nu$ = scan rate.

(3) Geiger, W. E.; Salzer, A.; Edwin, J.; von Philipsborn, W.; Piantini, U.; Rheingold, A. L. *J. Am. Chem. Soc.* **1990**, *112*, 7113.

(4) Rhodes, M. R.; Mann, K. R. *Inorg. Chem.* **1984**, *23*, 2053.

(5) Smith, D. A.; Zhuang, B.; Newton, W. E.; McDonald, J. W.; Schultz, F. A. *Inorg. Chem.* **1987**, *26*, 2524.

(6) Koide, Y.; Bautista, M. T.; White, P. S.; Schauer, C. K. *Inorg. Chem.* **1992**, *31*, 3690.

(7) Collman, J. P.; Rothrock, R. K.; Finke, R. G.; Moore, E. J.; Rose-Munch, F. *Inorg. Chem.* **1982**, *21*, 146.

(8) Connelly, N. G.; Lucy, A. R.; Payne, J. D.; Galas, A. M. R.; Geiger, W. E. *J. Chem. Soc., Dalton Trans.* **1983**, 1879.

(9) Fernandes, J. B.; Zhang, L. Q.; Schultz, F. A. *J. Electroanal. Chem.* **1991**, *297*, 145.

(10) Lockemeyer, J. R.; Rauchfuss, T. B.; Rheingold, A. L. *J. Am. Chem. Soc.* **1989**, *111*, 5733.

(11) Finke, R. G.; Voegeli, R. H.; Laganis, E. D.; Boekelheide, V. *Organometallics* **1983**, *2*, 347.

(12) (a) Bowyer, W. J.; Merkert, J. W.; Geiger, W. E. *Organometallics* **1989**, *8*, 191. (b) Bowyer, W. J.; Geiger, W. E. *J. Electroanal. Chem.* **1988**, *239*, 253.

(13) Thompson, R. L.; Geib, S. J.; Cooper, N. J. *J. Am. Chem. Soc.* **1991**, *113*, 8961.

(14) Rieke, R. D.; Arney, J. S.; Rich, W. E.; Willeford, B. R., Jr.; Poliner, B. S. *J. Am. Chem. Soc.* **1975**, *97*, 5951.

(15) Pierce, D. T.; Geiger, W. E. *J. Am. Chem. Soc.* **1992**, *114*, 6063.

S0002-7863(96)00259-4 CCC: $12.00 

allow facile formation and cleavage of linkages as strong as C−C bonds.[3] A major focus has been on questions of whether the electron transfer (et) and structure change are separate (as in ECE-type mechanisms) or concerted (an EE mechanism) and whether the dominant structural change is coupled to the first or to the second charge transfer.[16] Quantitative treatments of two-electron processes in compounds with specific geometric and electronic features will aid in evaluation of the models emerging to account for multielectron reactions. Especially intriguing is the possibility of deriving estimates for strengths of bonds broken in these reactions,[17] by analogy with theories successfully implemented for one-electron processes.[18]

Redox processes involving the chemically reversible fracture of metal−metal bonds may provide a fertile ground for testing electron-transfer models. Since fulvalenediyl dimetallic complexes are capable of undergoing such processes,[8,19−21] they are of continuing interest in this regard. $C_{10}H_8$-bridged dimetallic complexes prefer an *anti* arrangement of the metals if metal−metal bond formation is not required for the metals to achieve 18-electron configurations. Electronically-unsaturated metals (e.g., 17-electron metals) may form *syn* complexes with M−M bonds[22] if the metals carry nonsterically demanding ligands and if the half-filled orbitals of the 17-electron metals are oriented along the putative M−M bond.[23,24]


*syn* *anti*

Relevant to this discussion is the behavior of the *syn* complexes $Fv[M(CO)_3]_2$, (M = Cr, Mo, W), **3**, which reduce cleanly to *anti*-$\{Fv[M(CO)_3]_2\}^{2-}$, **4**, in two-electron voltammetric waves; complexes **3** are quantitatively regenerated through oxidation of the dianions, **4** (eq 4).[19] The reduction

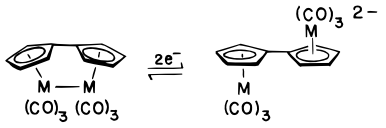


**3** **4** (4)

and reoxidation processes each take place in single two-electron cathodic and anodic waves at the potentials $E_{pc}$ and $E_{pa}$, respectively. The separation of the two waves, $\Delta E_p$ (= $E_{pa}$ − $E_{pc}$), varies greatly with the identity of the metal: 150 mV for M = Cr, ca. 700 mV for M = Mo, W. This finding was rationalized on the basis of metal−metal bond strengths in the series, which are expected to follow the trend Cr−Cr < Mo−Mo < W−W.[19]

The proposed correlation of larger $\Delta E_p$ values with systems having stronger M−M bonds is not supported by the results of Pugh and Meyer.[17] These authors studied a series of dinuclear compounds including bis(cyclopentadienyl) metal complexes such as $[Cp_2Mo_2(CO)_6]$, **5**, and $[Cp_2Fe_2(CO)_4]$ which reduce to two mononuclear anions with cleavage of a metal−metal bond (eq 5), the formal equivalent of **3** + 2e⁻ ⇌ **4**.

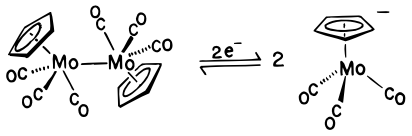


**5** **6** (5)

A pattern of one irreversible cathodic wave (e.g., **5** + 2e⁻ ⇌ 2$[CpMo(CO)_3]^-$) and one irreversible anodic wave (2**6** ⇌ **5** + 2e⁻) was found, similar to that seen for the analogous fulvalenediyl complexes.[19] In this case, however, the $\Delta E_p$ separation did *not* correlate with trends in M−M bond strength.

There are two important differences in the M−M bond formation steps of the two sets of redox pairs in eqs 4 and 5: (1) an *intra*molecular process is involved for **3**/**4**, compared to an *inter*molecular one in **5**/**6** and (2) a *syn*/*anti* rotation around the hydrocarbon bridge is required in **3**/**4**. In this light, we thought it of interest to test the voltammetric behavior of two closely-related structures, both of which undergo reversible intramolecular M−M bond cleavage but only one of which requires rotation around the $C_{10}H_8$ linkage. The complexes **1** and **2** fulfill these requirements. The dication $\mathbf{2}^{2+}$ has a metal−metal bond length [2.837(1) Å] consistent with a normal Rh−Rh bond, whereas the Rh···Rh separation in neutral **2** [4.511(1) Å] precludes a significant bonding interaction (*vide infra*). The dication $\mathbf{1}^{2+}$ was too unstable to be similarly characterized by crystallography, but its optical and infrared spectra were consistent with the presence of a Rh−Rh bond, as found also in the close structural analogue $[(Fv)Rh_2(CO)_2(PPh_3)_2]^{2+}$ ($d_{Rh-Rh}$ = 2.930 Å).[24] Compound **1**, which was previously shown to be oxidizable with ferrocenium ion,[21] was chosen for a detailed voltammetric study because its relatively small carbonyl ligands present minimum steric encumberance to fulvalenediyl rotation. Idealized structures for the anodic redox processes of $\mathbf{1}/\mathbf{1}^{2+}$ and $\mathbf{2}/\mathbf{2}^{2+}$ are shown in eqs 6 and 7, respectively.

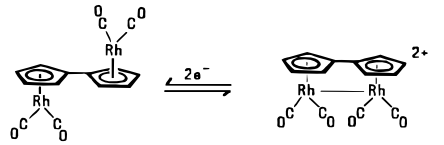


(6)

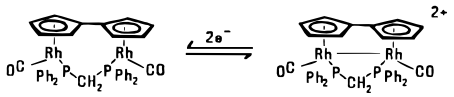


(7)

The time dependence of the voltammetric behavior of **1** and **2** opens opportunities for quantitative characterization of the electron-transfer mechanisms. In spite of the geometric changes involved, close-to-Nernstian behavior is observed for the oxidation of both **1** and **2** at slow CV sweep rates. At higher sweep rates, deviations from electrochemical reversibility are found which enable us to diagnose the rate-determining et step and to estimate the thermodynamic and kinetic factors associated with the two-electron processes. The $\Delta E_p$ values are much smaller than those predicted by a model correlating $\Delta E_p$ with metal−metal bond dissociation energy.[19] The effect of ful-

(16) For leads to CEE, ECE, and EEC processes, see refs 28−43 of ref 15.

(17) Pugh, J. R.; Meyer, T. J. *J. Am. Chem. Soc.* **1992**, *114*, 3784.

(18) (a) Saveant, J. M. In *Advances in Electron Transfer Chemistry*; Mariano, P. S., Ed.; JAI Press: New York, 1994; Vol. 4, p 53. (b) Andrieux, C. P.; Robert, M.; Saveant, J.-M. *J. Am. Chem. Soc.* **1995**, *117*, 9340 and references therein.

(19) Moulton, R.; Weidman, T. W.; Vollhardt, K. P. C.; Bard, A. J. *Inorg. Chem.* **1986**, *25*, 1846.

(20) Brown, D.; Delville-Desbois, M. H.; Vollhardt, K. P. C.; Astruc, D. *New J. Chem.* **1992**, *16*, 899.

(21) Bitterwolf, T. E.; Spink, W. C.; Rausch, M. D. *J. Organomet. Chem.* **1989**, *363*, 189.

(22) Vollhardt, K. P. C.; Weidman, T. W. *Organometallics* **1984**, *3*, 82 and references therein.

(23) One fulvalenediyl complex with two 17-electron metals which most likely has an *anti* orientation is the biferrocenium dication: (a) Morrison, W. H., Jr.; Hendrickson, D. N. *J. Chem. Phys.* **1973**, *59*, 380. (b) Levanda, C.; Bechgaard, K.; Cowan, D. O. *J. Org. Chem.* **1976**, *41*, 2700. For a summary of redox chemistry in fulvalenediyl complexes, see; Astruc, D. *Electron Transfer and Radical Processes in Transition-Metal Chemistry*; VCH Publishers: New York, 1995; pp 154−60.

(24) Freeman, M. J.; Orpen, A. G.; Connelly, N. G.; Manners, I.; Raven, S. J. *J. Chem. Soc., Dalton Trans.* **1985**, 2283.

valenediyl rotation is seen, however, in a lowering of the et rate of **1** compared to that of **2**.

## Experimental Section

**Chemicals.** (Fv)$Rh_2(CO)_4$, **1**, and (Fv)$Rh_2(CO)_2(\mu$-dppm), **2**, were prepared according to literature methods[21,25] and identified by $^1$H NMR and IR measurements. All solvents were dried and distilled under nitrogen, and standard Schlenk procedures were employed throughout.

Reagent-grade dichloromethane used for electrochemistry was first distilled from $CaH_2$. Acetone distilled from $CaSO_4$ and nitromethane treated with type 4A molecular sieves gave clean voltammetric backgrounds in the regions of interest. $[Bu_4N][PF_6]$ was prepared by metathesis of $[Bu_4N]I$ and $[NH_4][PF_6]$, recrystallized from 95% ethanol, and vacuum dried. $[Cp_2Fe][PF_6]$ was prepared through the oxidation of sublimed ferrocene by $Ag[PF_6]$ in $CH_2Cl_2$.

**Preparation of Dicationic Complexes.** Both dications, $[\mathbf{1}][PF_6]_2$ and $[\mathbf{2}][PF_6]_2$, were previously reported.[21] Since the material we obtained as $[\mathbf{1}][PF_6]_2$ has somewhat different characteristics than that obtained after longer reaction times,[21] we offer complete details of our preparations.

The dication $\mathbf{1}^{2+}$ was prepared as the bis-hexafluorophosphate salt by oxidation of **1** with 2 equiv of $[Cp_2Fe][PF_6]$. A stirred solution of **1** (19 mg, 0.042 mmol) in 10 mL of $CH_2Cl_2$ was stirred at 273 K with $[Cp_2Fe][PF_6]$ (28 mg, 0.085 mmol) until the reaction was complete (ca. 10 min) as judged by IR spectroscopy following the disappearance of the 2039 and 1978 cm$^{-1}$ bands of **1**. Longer reaction times led to extensive decomposition of $\mathbf{1}^{2+}$. The green solid was washed with diethyl ether (3 × 10 mL), dried *in vacuo* at 273 K for 2 h, and stored under $N_2$ at 250 K. $[\mathbf{1}][PF_6]_2$ is quite unstable in solution at ambient temperatures; voltammetry of the dication was obtained after dissolving the dication in cold acetone solutions. Likewise, IR spectra obtained at subambient temperatures show bands at 2146 and 2114 cm$^{-1}$, attributed to the carbonyls of $\mathbf{1}^{2+}$, but at higher temperatures bands near 2128 and 2099 cm$^{-1}$ grew in which had earlier been attributed to $\mathbf{1}^{2+}$.[21] IR spectroelectrochemical experiments (see below) establish that the latter pair of bands arises from the decomposition of $\mathbf{1}^{2+}$.

The oxidation of **2** followed the same procedure as given above for **1** and gave an analytically pure sample of $[\mathbf{2}][PF_6]_2$ (40% yield, recrystallized from acetone/diethyl ether) with IR and $^1$H NMR data in complete accord with those in the literature.[21] X-ray quality crystals were grown from acetone/diethyl ether at 243 K under $N_2$.

**Electrochemical Procedures.** Standard electrochemical techniques were employed using cells housed inside a drybox under nitrogen. Temperature control was achieved by immersing the cell in a heptane bath controlled to ±1° by an FTS temperature control system. In bulk electrolyses the working and auxiliary compartments were separated by two fine-porosity frits to assure separation of the anolyte and catholyte. The supporting electrolyte was 0.1 M $[Bu_4N][PF_6]$. The experimental reference electrode was Ag/AgCl, prepared by anodizing a silver wire in aqueous HCl. Since Ag/AgCl does not exhibit great stability in some nonaqueous solvents, ferrocene was always added at an appropriate point in the experiment to serve as an internal standard. All potentials in this paper are referenced to the ferrocene/ferrocenium (Fc) couple. Comparisons to couples reported vs the aqueous SCE reference require the addition of 0.46 V ($CH_2Cl_2$) or 0.48 V (acetone) to the potentials *vs* Fc. Pt, Au, and glassy carbon disks (Bioanalytical Systems) were used as working electrodes in most voltammetry experiments. Some use was made of hanging mercury drop electrodes. The solid electrodes were pretreated by hand polishing them on microcloth with a series of diamond pastes of diminishing diameters, finishing with 0.25 $\mu$m. Identical CV traces were obtained on Pt disks treated by this method and on Pt bead electrodes pretreated by a chemical oxidation ($HNO_3$)/reduction ($Fe^{2+}$) cycle. A cylindrical Pt gauze served as the working electrode for bulk electrolyses. Digital simulation of cyclic voltammograms by the explicit finite difference method[26] used homewritten programs executed on personal computers.

(25) Rausch, M. D.; Spink, W. C. *J. Organomet. Chem.* **1986**, *308*, C1.

(26) Feldberg, S. W. In *Electroanalytical Chemistry*; Bard, A. J., Ed.; Marcel Dekker: New York, 1969; Vol. 3, p 199. Copies of these programs (in Fortran) may be obtained from the corresponding author.

**Table 1.** Crystal Data for **2** and $[\mathbf{2}][PF_6]_2$·Acetone (Radiation = Mo Kα ($\lambda$ = 0.710 73 Å)

| | **2** | $\mathbf{2}^{2+}$ |
|---|---|---|
| formula | $C_{27}H_{30}O_2P_2Rh_2$ | $C_{37}H_{30}F_{12}O_2P_4Rh_2$·$C_3H_6O$ |
| formula weight | 774.4 | 1122.4 |
| space group | $P\bar{1}$ | $Pca2_1$ |
| *a*, Å | 9.620(3) | 17.576(2) |
| *b*, Å | 11.169(3) | 13.849(2) |
| *c*, Å | 15.566(6) | 17.794(3) |
| α, deg | 86.52(3) | |
| $\beta$, deg | 74.15(3) | |
| $\gamma$, deg | 74.75(2) | |
| *V*, Å$^3$ | 1552.1(9) | 4331.1(12) |
| *Z* | 2 | 4 |
| cryst dimens, mm | 0.16 × 0.18 × 0.28 | 0.18 × 0.30 × 0.32 |
| cryst color | brown | orange-yellow |
| *D*(calc), g cm$^{-3}$ | 1.657 | 1.722 |
| $\mu$(Mo Kα), cm$^{-1}$ | 12.00 | 10.00 |
| indpt reflns | 7118 | 3531 |
| *R*(*F*), % | 3.73 | 8.07 |
| $R_w$(*F*), % | 4.56 | 9.39 |

**Instrumentation.** Electrochemical experiments were conducted using a PARC model 173 potentiostat, and voltammograms were recorded on either a Hewlett-Packard model 7046B X−Y recorder or on a Nicolet 4094A digital oscilloscope. Approximate elimination of the charging current was achieved in higher scan rate experiments by digital subtraction of the background blank. Infrared spectroelectrochemistry was conducted in an OTTLE cell described elsewhere[27] at temperatures between ambient and 243 K. IR spectra were recorded with a Mattson Polaris IR spectrometer at 2 cm$^{-1}$ resolution. UV−VIS spectra were recorded with a Perkin-Elmer Lambda 6 spectrophotometer. To obtain an optical spectrum of $\mathbf{1}^{2+}$, the ambient-temperature solutions of which are unstable, a Nujol mull of the solid sample was pasted onto a soft tissue (Kimwipe) cut to a size to fit on the inside window of a quartz UV−VIS cell.

**Structure Determinations of 2 and $\mathbf{2}^{2+}$.** Crystallographic data on **2** and $[\mathbf{2}][PF_6]_2$·acetone are collected in Table 1. Both were mounted in glass capillaries and photographically characterized. Laue symmetries $\bar{1}$ and *mmm* were found, respectively. For **2** the centrosymmetry assumed throughout was supported by the well-behaved refinement. For $\mathbf{2}^{2+}$ systematic absences in the diffraction data indicated either of the orthorhombic space groups $Pca2_1$ or *Pcam*. The *E*-statistics initially suggested the noncentrosymmetric alternative, and this was confirmed by the inability of the structure to possess mirror-plane symmetry. $\psi$-scan data showed less than 10% variation, and corrections for absorption were ignored.

The Rh atoms were located by direct methods, and the structures were completed from subsequent difference maps. In $\mathbf{2}^{2+}$, one molecule of acetone for each ion pair was also located in the lattice. All non-hydrogen atoms were anisotropically refined, and hydrogen atoms were idealized. All computations used SHEXTL (4.2) software (G. Sheldrick, Siemens XRD, Madison, WI). Some noteworthy bond lengths, atom−atom distances, and bond angles of **2** and $\mathbf{2}^{2+}$ are collected in Table 2.

## Results

**R.I. Oxidation of 1 and Identification of Oxidation Product $\mathbf{1}^{2+}$.** Quasi-reversible two-electron waves are seen for the oxidation of (Fv)$Rh_2(CO)_4$, **1**, at Pt or glassy carbon electrodes in $CH_2Cl_2$, $CH_3NO_2$, and acetone with an $E_{1/2}$ value of ca. −0.12 V calculated from the average of the anodic and cathodic peak potentials at low scan rates. Since chronoamperometry experiments showed that the anodic product $\mathbf{1}^{2+}$ adsorbs strongly to Pt in $CH_2Cl_2$,[28] quantitative voltammetry was carried

(27) Atwood, C. G.; Geiger, W. E.; Bitterwolf, T. E. *J. Electroanal. Chem.* **1995**, *397*, 279.

(28) Double-potential step chronoamperometry (−0.4 to 0.2 to −0.4 V, step time $\tau$ = 5 s) in $CH_2Cl_2$ revealed a value for $i(2\tau)/i(\tau)$ of 0.58, higher than the 0.29 expected[29] for a soluble electrode product. This behavior is diagnostic of electrode product film formation at the electrode surface.

**Table 2.** Selected Bond Distances and Angles for **2** and $\mathbf{2}^{2+}$

| | **2** | $\mathbf{2}^{2+}$ |
|---|---|---|
| (a) Bond Distances (Å) | | |
| CNT−Rh(1) | 1.966(2) | 1.834(2) |
| CNT−Rh(2) | 1.934(2) | 1.842(2) |
| Rh(1)−Rh(2) | 4.511(1) | 2.837(1) |
| Rh(1)−P(1) | 2.264(1) | 2.293(4) |
| Rh(2)−P(2) | 2.235(1) | 2.298(5) |
| Rh(1)−C(1) | 1.815(5) | 1.86(2) |
| Rh(2)−C(2) | 1.813(5) | 1.93(2) |
| (b) Bond Distances (deg) | | |
| CNT−Rh(1)−P(1) | 137.8(2) | 130.0(3) |
| CNT−Rh(2)−P(2) | 132.3(2) | 128.1(4) |
| CNT−Rh(1)−C(1) | 132.8(4) | 128.3(5) |
| CNT−Rh(2)−C(2) | 135.8(4) | 131.4(5) |
| P(1)−Rh(1)−C(1) | 89.2(1) | 93.6(6) |
| Rh(1)−P(1)−C(13) | 122.1(1) | 111.0(5) |
| Rh(2)−P(2)−C(13) | 113.0(1) | 110.6(5) |
| P(1)−C(13)−P(2) | 118.3(2) | 112.6(10) |
| (c) Torsional, Dihedral Angles (deg) | | |
| CNT−C(7)−C(8)−CNT | 6.9 | 21.0 |
| CNT−Rh(1)−Rh(2)−CNT | 16.2 | 5.0 |
| P(1)−Rh(1)−Rh(2)−CNT | 59.4 | 5.3 |
| [C(3) to C(7)]−[C(8) to C(12)] | 21.3 | 26.8 |

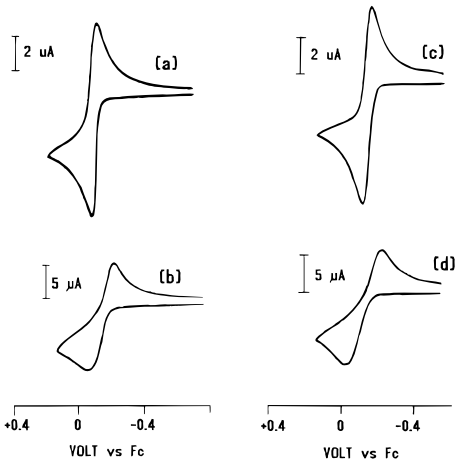


**Figure 1.** CV scans of **1** at 298 K, Pt electrode. Left: 0.64 mM in $CH_3NO_2$ (a) $\nu = 0.1$ V/s (b), $\nu = 0.4$ V/s. Right: 0.50 mM in acetone (c) $\nu = 0.1$ V/s, (b) $\nu = 0.4$ V/s.

out in nitromethane and acetone, in which the dication is soluble. Because the behavior of **1** in the latter two solvents was virtually identical (Figure 1), only the data in acetone are discussed. Some important voltammetric data are listed in Table 3.

At ambient temperatures and slow CV sweep rates, the oxidation and reduction waves are symmetrically shaped and display quasi-Nernstian diagnostics. The peak separation $\Delta E_p$ ($= E_{pa} - E_{pc}$) was ca. 50 mV at low $\nu$ and increased with scan rate. The breadth of the anodic peak $\delta E_p$ ($= E_p - E_{p/2}$) was 45−50 mV. Both $\Delta E_p$ and $\delta E_p$ have values between those expected for Nernstian one- and two-electron processes. The stoichiometry of the anodic process was established as two electrons by (a) comparison of the electrochemical responses of **1** with those of equimolar decamethylferrocene regarding (i) ratio of anodic peak current functions, $i_p/\nu^{1/2}$ (1.8), (ii) voltammetry at the rotating Pt electrode (ratio of limiting plateau currents, 1.9), and (iii) chronoamperometry at a Pt disk electrode (ratio of values of $it^{1/2} = 2.0$ for $t = 5$ s) and (b) bulk coulometry (2.0 F). Assuming a two-electron transfer, the diffusion coefficient of **1** in acetone at 298 K is $1.31 \times 10^{-5}$ cm$^2$ s$^{-1}$ (calculated from chronoamperometric data).

That the dication $\mathbf{1}^{2+}$ partially decomposes at room temperature on the voltammetric time scale is best indicated by reverse chronoamperometry on **1** (double-potential step chronoamperometry) in which the potential is stepped from −0.7 to 0.2 to −0.7 V with a 5 s step time. For a chemically reversible process, the ratio of the current at the end of the reverse (cathodic) step to that at the end of the forward (anodic) step is 0.29 in theory[29] and 0.26−0.28 for model systems (e.g., ferrocene) under our experimental conditions. Our measurement of 0.22 for the $\mathbf{1}/\mathbf{1}^{2+}$ couple implies that the dication is somewhat unstable at 298 K.

Bulk electrolysis in acetone at 243 K ($E_{appl} = 0.4$ V) released 2.0 F per equivalent of **1** as the solution changed from orange to yellow-green. Re-electrolysis of the dication at $E_{appl} = -0.6$ V (1.8 F) resulted in a 96% regeneration of **1**, showing that $\mathbf{1}^{2+}$ is stable at this temperature over ca. 20 min. The above data are all consistent with eq 8 describing the anodic fate of **1**.

$$(Fv)Rh_2(CO)_4 \rightleftharpoons 2e^- + [(Fv)Rh_2(CO)_4]^{2+} \rightarrow \text{slow dec} \qquad (8)$$

Chemical oxidation of **1** by 2 equiv of [CpFe][$PF_6$] allowed isolation of a green solid which displayed a $^1$H NMR spectrum in cold $d_6$-acetone identical to that previously assigned to $\mathbf{1}^{2+}$ (*t*, 6.02; *t*, 7.59).[21] Infrared spectra of the powder gave results different than those previously reported, however, and an infrared spectroelectrochemical experiment was conducted to settle the question of the IR spectrum of $\mathbf{1}^{2+}$. In the anodic electrolysis of 2 mM **1** in acetone at 243 K, $\nu_{CO}$ of **1** (2033, 1973 cm$^{-1}$) disappeared and a new pair of absorptions arose at 2146 and 2114 cm$^{-1}$ (Figure 2). Since increases in excess of 100 cm$^{-1}$ are typical of metal carbonyls undergoing an increase of one in the metal oxidation states,[30] the bands at 2146 and 2114 cm$^{-1}$ are assigned to $\mathbf{1}^{2+}$. Cathodic re-electrolysis of $\mathbf{1}^{2+}$ gave back the spectrum of **1** in 67% yield. Because the features previously attributed to $\mathbf{1}^{2+}$ (2128, 2099 cm$^{-1}$)[21] were obtained if the oxidation of **1** were performed at ambient temperatures or cold electrolysis solutions of $\mathbf{1}^{2+}$ were warmed, these features appear to arise from secondary products.

The possibility of a metal−metal bond in $\mathbf{1}^{2+}$ was probed by optical spectroscopy, since the dication was too unstable to yield X-ray quality crystals. $d^7$−$d^7$ systems containing a single M−M bond exhibit an intense $\sigma/\sigma^*$ transition in the range 20000−30000 cm$^{-1}$.[31,32] The solid complex [**1**][$PF_6$]$_2$ in Nujol gave such an absorption at 25 190 cm$^{-1}$ (Figure 3) (Table 4).[33] The metal−metal bonded structure idealized in eq 6 is therefore assigned to $\mathbf{1}^{2+}$.

**R.II. Detailed Voltammetric Analysis of $\mathbf{1}/\mathbf{1}^{2+}$.** At increased CV sweep rates, the anodic wave for the oxidation of **1** broadened compared to the cathodic wave coupled to it (Figure 1). This is diagnostic of a rate-limiting *first* electron transfer when applied to an EE mechanism.[34] The general morphology of the CV curves remains unchanged to sweep rates in excess of 100 V/s, and no new features are observed that might be

(29) Schwarz, W. M.; Shain, I. *J. Phys. Chem.* **1965**, *69*, 30.
(30) Nakamoto, K. *Infrared and Raman Spectra of Inorganic and Coordination Compounds*, 4th ed.; John Wiley: New York, 1986; pp 291−295.
(31) Geoffroy, G. L.; Wrighton, M. S. *Organometallic Photochemistry*; Academic Press: New York, 1979; pp 20−22.
(32) (a) Levenson, R. A.; Gray, H. B.; Caesar, G. P. *J. Am. Chem. Soc.* **1970**, *92*, 3653. (b) Levenson, R. A.; Gray, H. B. *J. Am. Chem. Soc.* **1975**, *97*, 6042. (c) Jackson, R. A.; Poe, A. *Inorg. Chem.* **1978**, *17*, 997.
(33) As a check on the technique (Nujol mull on Kimwipe), we recorded the UV−VIS spectrum of [$CpMo(CO)_3$]$_2$, for which a $\sigma \rightarrow \sigma^*$ absorption energy of $25.8 \times 10^3$ cm$^{-1}$ had been reported in an EPA glass (Wrighton, M. S.; Ginley, D. S. *J. Am. Chem. Soc.* **1975**, *97*, 4246). The band position was at $25.2 \times 10^3$ cm$^{-1}$ in Nujol.
(34) Ryan, M. D. *J. Electrochem. Soc.* **1978**, *125*, 547.

**Table 3.** Representative Cyclic Voltammetric Data for Compounds **1**, $\mathbf{1}^{2+}$, **2**, and $\mathbf{2}^{2+}$ at Pt Electrode, $T$ = Ambient (Except $\mathbf{1}^{2+}$, $T$ = 243 K)

| compd | process | solv | $E_{pa}$ (V) | $E_{pc}$ (V) | $E^{\circ\prime}_{app}$ (V) | $\Delta E_p$ (mV) | $\delta E_p$ (mV) | $i_c/i_a$ | $\nu$ (V/s) |
|---|---|---|---|---|---|---|---|---|---|
| **1** | oxdn | $CH_3NO_2$ | −0.110 | −0.166 | −0.14 | 56 | | 0.99 | 0.10 |
| **1** | oxdn | $CH_3NO_2$ | −0.016 | −0.210 | −0.11 | 194 | | 1.05 | 0.40 |
| **1** | oxdn | acetone | −0.078 | −0.160 | −0.12 | 82 | 47 | 1.0 | 0.05 |
| $\mathbf{1}^{2+}$ | redn | acetone | | | −0.20 | 300 | | | 0.20 |
| **2** | oxdn | $CH_2Cl_2$ | −0.728 | −0.772 | −0.75 | 44 | 34 | 1.0 | 0.10 |
| $\mathbf{2}^{2+}$ | redn | $CH_2Cl_2$ | −0.729 | −0.772 | −0.75 | 46 | 36 | | 0.05 |

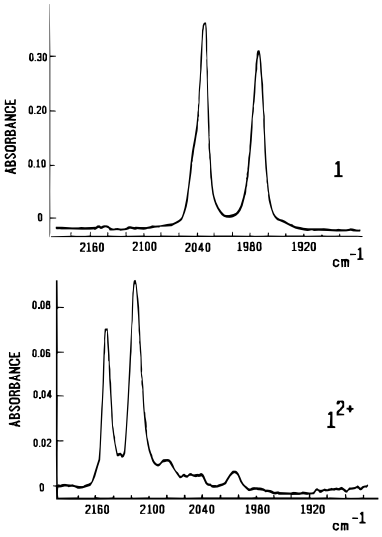


**Figure 2.** IR spectroelectrochemistry of 2 mM **1** in acetone/0.5 M $[NBu_4][PF_6]$ at 243 K: (top) before electrolysis; (bottom) after anodic electrolysis at $E_{appl} = +0.2$ V.

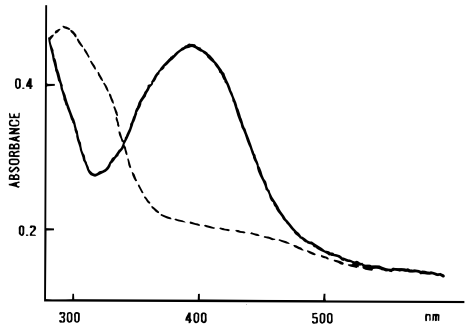


**Figure 3.** Optical spectra of **1** (dashed line) and $[\mathbf{1}][PF_6]_2$ as solids dispersed in Nujol.

**Table 4.** Optical Absorption Bands Attributed to $\sigma \rightarrow \sigma^*$ Transitions

| compd | medium | $\lambda_{max}$ (nm) | energy ($cm^{-1}$) | ref |
|---|---|---|---|---|
| $[\mathbf{1}][PF_6]_2$ | Nujol | 397 | $25.2 \times 10^3$ | this work |
| $[\mathbf{2}][PF_6]_2$ | Nujol | 416 | $24.0 \times 10^3$ | this work |
| $[FvRh_2(CO)_2(PPh_3)_2]^{2+}$ | Nujol | 403 | $24.8 \times 10^3$ | this work[a] |
| $FvRu_2(CO)_4$ | isooctane | 332 | $30.1 \times 10^3$ | 22 |
| $Mn_2(CO)_{10}$ | pentanes | 342 | $29.2 \times 10^3$ | 32 |
| $Mn_2(CO)_8(PPh_3)_2$ | $CH_3CN$ | 373 | $26.8 \times 10^3$ | 32 |

[a] complex prepared according to procedure in ref 24.

ascribed to intermediates. Lacking evidence for an ECE or EEC mechanism, we therefore treat the system with an EE mechanism, wherein structure changes and electron-transfer exchanges are concomitant. CV responses are in quantitative agreement with this model.

Figure 4 demonstrates the comparison between observed and theoretical voltammograms for $\mathbf{1}/\mathbf{1}^{2+}$. Optimum agreement was obtained with two separate et reactions separated by ca. 140 mV, with the $\mathbf{1}^{+}/\mathbf{1}^{2+}$ couple (eq 10) being *negative* of the $\mathbf{1}/\mathbf{1}^{+}$ couple (eq 9):

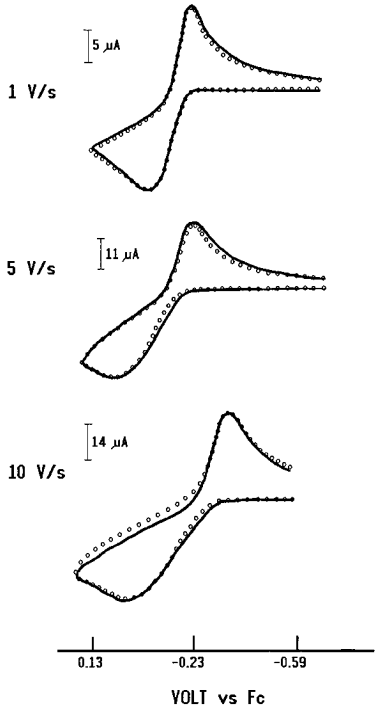


**Figure 4.** CV of 0.44 mM **1** in acetone at Pt, $T = 298$ K. Comparison of experimental data (circles) with simulations (solid lines) for EE mechanism at different scan rates. Simulation parameters in Table 5.

**Table 5.** Average of Best Simulation Fits Describing Voltammetric Parameters for Compounds **1**, **2** and $\mathbf{2}^{2+}$ in Acetone at Pt Electrode, $T$ = Ambient, Potentials vs Fc

| compd | couple | $E^{\circ\prime}$ (V) | $k_s$ (cm/s) | α | $(1-\alpha)$ | $\Delta G^{\ddagger}_{o}$[a] |
|---|---|---|---|---|---|---|
| **1** | 0/1+ | $-0.10_3$ | 0.013 | | 0.66 | 7.9 |
| **1** | 1+/2+ | $-0.24_5$ | 0.044 | 0.50 | | 7.3 |
| **2** | 0/1+ | $-0.76_2$ | 0.035 | | 0.75 | 7.6 |
| **2** | 1+/2+ | $-0.77_6$ | >0.2 | 0.50 | | <6.4 |
| $\mathbf{2}^{2+}$ | 2+/1+ | $-0.78_5$ | >0.15 | 0.50 | | |
| $\mathbf{2}^{2+}$ | 1+/0 | $-0.76_0$ | 0.020 | | 0.70 | |

| overall couple | $E^{\circ\prime}_{avg}$ (V) | $E^{\circ\prime}_{2+/1+} - E^{\circ\prime}_{1+/0}$ (V) |
|---|---|---|
| $\mathbf{1} \rightleftharpoons \mathbf{1}^{2+} + 2e^-$ | −0.17 | −0.14 |
| $\mathbf{2} \rightleftharpoons \mathbf{2}^{2+} + 2e^-$ | −0.77 | $-0.01_4$ |
| $\mathbf{2}^{2+} + 2e^- \rightleftharpoons \mathbf{2}$ | −0.77 | $-0.02_5$ |

[a] Electron-transfer activation barrier (in kcal/mol) calculated from $k_s = \kappa Z \exp\{-\Delta G^*_o/kT\}$ assuming adiabatic charge transfer ($\kappa = 1$) and a collision velocity ($Z$) of $10^4$ cm/s.

$$\mathbf{1} \rightleftharpoons \mathbf{1}^{+} + e^- \qquad E^{\circ\prime}_1, k_{s1}, (1-\alpha_1) \tag{9}$$

$$\mathbf{1}^{+} \rightleftharpoons \mathbf{1}^{2+} + e^- \qquad E^{\circ\prime}_2, k_{s2}, (1-\alpha_2) \tag{10}$$

The values for the et parameters obtained by averaging the parameters in the caption of Figure 4 are given in Table 5. The $E^{\circ\prime}$ values were fixed by two observables: a close estimate of $(E^{\circ\prime}_1 + E^{\circ\prime}_2)/2$ is obtained from the average of the cathodic

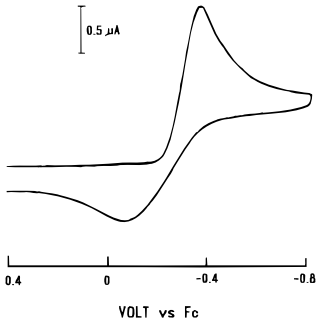


**Figure 5.** CV of [**1**][$PF_6$]$_2$ in acetone, $T$ = 243 K, Pt electrode, $\nu$ = 0.2 V/s.

and anodic peak potentials at very low $\nu$[35] and ($E^{\circ\prime}_2 - E^{\circ\prime}_1$) is obtained from the anodic peak breadth at very low $\nu$.[36] The transfer coefficient $\alpha_2$ was held at 0.5 in the simulations. Note that we define the transfer coefficient as $\alpha$ for a cathodic process and $(1 - \alpha)$ for an anodic process to avoid confusion with the complementary reactions when the dication $\mathbf{1}^{2+}$ (or $\mathbf{2}^{2+}$) is reduced (see below). Although other combinations of parameters might conceivably fit the observed voltammograms, it became clear through a large number of calculations that two quasi-reversible one-electron reactions, separated by about 140 mV, with the $\mathbf{1}/\mathbf{1}^{+}$ charge transfer being *slower* than that of $\mathbf{1}/\mathbf{1}^{2+}$, are required to fit the data.

**R.III. Qualitative Voltammetry of $\mathbf{1}^{2+}$.** Solutions of $\mathbf{1}^{2+}$ were prepared either by low-temperature anodic electrolysis of **1** or by dissolving the green solid [**1**][$PF_6$]$_2$ in cold acetone. The CV behavior of the dication (Figure 5) was complementary to that of the neutral complex in that it displays an anodic branch broader than the cathodic branch, consistent with a quasi-reversible two-electron reduction in which the slow step is the *second* charge transfer (that is, the reduction of $\mathbf{1}^{+}$ to **1**). Quantitative CV investigations were left to the dication $\mathbf{2}^{2+}$, which was more stable than $\mathbf{1}^{2+}$ under the conditions employed (see below).

**R.IV. Oxidation of 2 and Characterization of $\mathbf{2}^{2+}$.** The doubly-bridged complex **2** undergoes a quasi-Nernstian two-electron oxidation to a stable dication.[21] Electrochemical measurements show that the transformation $\mathbf{2}/\mathbf{2}^{2+}$ is highly efficient in dichloromethane. A single oxidation wave is observed (apparent $E^{\circ\prime} = -0.75$ V) with a peak current 1.8 times the height of equimolar ferrocene (Figure 6).[37] Values of $\Delta E_p$ = 44 mV and $\delta E_p$ = 34 mV were observed with $\nu$ = 0.1 V/s at 298 K. The shape of the CV curve and its response to sweep rate changes will be discussed below. Double-potential step chronocoulometry (−1.2 to −0.4 to −1.2 V, step time 5 s) established the absence of specific adsorption of the electrode reactant and product, **2** and $\mathbf{2}^{2+}$, respectively.[38] From the chronoamperometric $it^{1/2}$ value, the diffusion coefficient of **2** was determined to be $8.67 \times 10^{-6}$ cm$^2$ s$^{-1}$ in $CH_2Cl_2$ at 298 K.

Bulk anodic electrolysis confirmed the two-electron stoichiometry ($n_{app}$ = 1.8 e$^-$, color change from orange to yellow-green, $E_{appl} = -0.50$ V, $T$ = 243 K in $CH_2Cl_2$). Back-reduction of $\mathbf{2}^{2+}$ at $E_{appl} = -1.0$ V regenerated **2** in >80% yield. IR

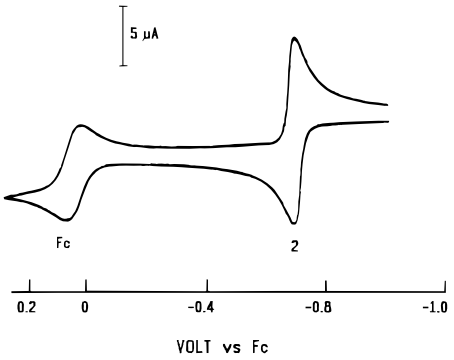


**Figure 6.** CV of 1.16 mM **2** and 1.08 mM ferrocene in $CH_2Cl_2$, $T$ = 298 K, Pt electrode, $\nu$ = 0.1 V/s.

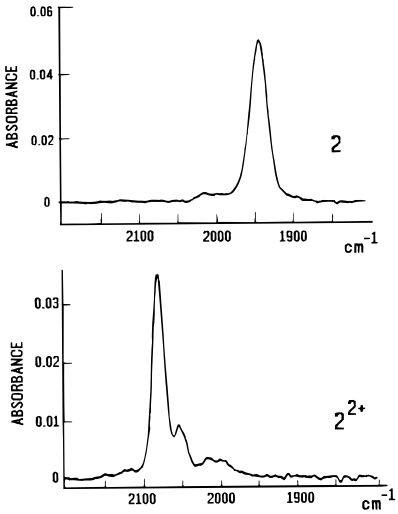


**Figure 7.** IR spectroelectrochemistry of 1.1 mM **2** in $CH_2Cl_2$ at $T$ = 243 K: (top) before electrolysis; (bottom) after anodic electrolysis at $E_{appl} = -0.3$ V.

sampling of the oxidized and reduced solutions confirmed the identity of the species involved (see IR results below). The original 1.04 mM solution of **2** gave a plateau anodic current of 23 $\mu$A with a rotating Pt electrode. The cathodic plateau current of only 13 $\mu$A after production of $\mathbf{2}^{2+}$ is not accounted for solely by 10−20% decomposition during the electrolysis; assuming that precipitation of the dication is not important (none was detected in visual inspections) this implies that the diffusion coefficient is appreciably lower for $\mathbf{2}^{2+}$ than for **2**. There is precedent for such an observation.[3,39,40] The diffusion coefficient of $\mathbf{2}^{2+}$ was later measured using samples of the pure dication as $5.62 \times 10^{-6}$ cm$^2$ s$^{-1}$.

The dication [**2**][$PF_6$]$_2$ was isolated by ferrocenium oxidation of **2**, as reported by others.[21] An IR spectroelectrochemistry experiment ($CH_2Cl_2$, 243 K) confirmed that neutral **2** ($\nu_{CO}$ = 1945 cm$^{-1}$) converted directly to $\mathbf{2}^{2+}$ upon oxidation. Although the major IR band in $\mathbf{2}^{2+}$ moves to 2082 cm$^{-1}$, a weak band at 2053 cm$^{-1}$ also appears to arise from the dication (Figure 7). Weak vibrational coupling between the two CO groups may arise from the presence of the metal−metal bond in the dication. Further spectroscopic evidence pointing to the existence of a Rh−Rh bond was obtained from the Nujol mull optical spectrum of the dication, from which a $\sigma \rightarrow \sigma^*$ transition was detected at 24 040 cm$^{-1}$. The red shift for $\mathbf{2}^{2+}$ compared to $\mathbf{1}^{2+}$ ($\sigma \rightarrow \sigma^*$ at 25 190 cm$^{-1}$, see above) is consistent with phosphine-for-carbonyl ligand substitution (Table 4).[32]

**R.V. X-ray Structural Analysis of $\mathbf{2}^{2+}$.** Structural studies prove that a Rh−Rh bond is absent in **2** (Figure 8, $d_{Rh-Rh}$ =

(35) Myers, R. L.; Shain, I. *Anal. Chem.* **1969**, *41*, 980.
(36) Richardson, D. E.; Taube, H. *Inorg. Chem.* **1981**, *20*, 1278.
(37) The lower diffusion coefficient of **2** (see text) compared to that of ferrocene assures that the current function for $\mathbf{2}/\mathbf{2}^{2+}$ will be less than twice that of ferrocene/ferrocenium. Values of 1.9 to 1.3 are predicted from the Randles−Sevcik equation depending on whether one or two electrons are transfered in the rate-determining step. The measured value of 1.8 may be taken as evidence for an overall two-electron process, but drawing further conclusions about the *n* value in the rate-determining et would, in our view, be speculative.
(38) Forward slope = $2.1 \times 10^{-4}$ C s$^{-1/2}$, intercept = 7.1 $\mu$C: reverse slope $1.9 \times 10^{-4}$ C s$^{-1/2}$, intercept = 7.1 $\mu$C.
(39) Edwin, J.; Geiger, W. E. *J. Am. Chem. Soc.* **1990**, *112*, 7104.
(40) Rongfeng, Z.; Evans, D. H. *J. Electroanal. Chem.* **1995**, *385*, 201.

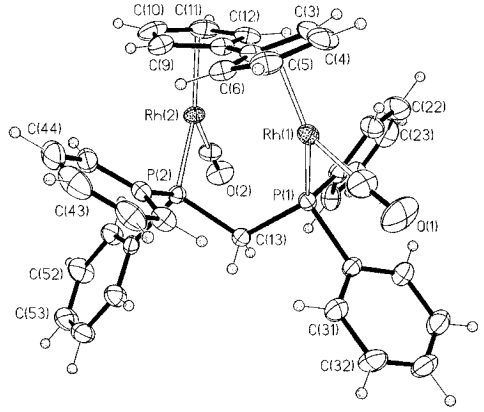


**Figure 8.** Molecular geometry of **2**.

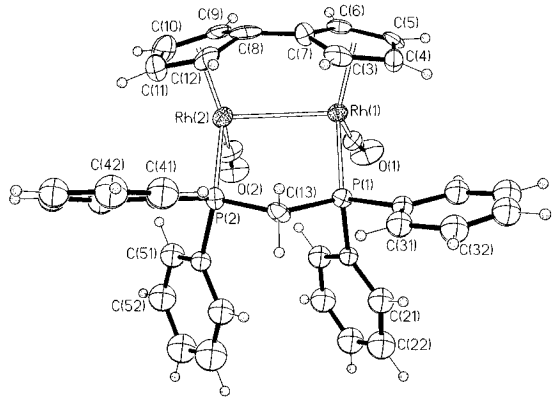


**Figure 9.** Molecular geometry of $\mathbf{2}^{2+}$ viewed perpendicular to the Rh−Rh bond.

4.511 Å) but present in $\mathbf{2}^{2+}$ (Figure 9, $d_{\mathrm{Rh-Rh}} = 2.837$ Å). The metal−metal distance in the latter is comparable to those observed in isoelectronic Rh[24] and Ru[41] systems. Another notable feature is that the formation of the Rh−Rh bond in the dication forces the dppm ligand to one side. In the neutral species the dppm ligand crosses the Rh···Rh vector. Distortion of the two cyclopentadienyl rings from coplanarity is higher in the dication (dihedral angle 21°) than in the neutral complex (6.9°).

**R.VI. Detailed Voltammetric Analysis of $\mathbf{2}/\mathbf{2}^{2+}$.** When solutions of **2** were subjected to CV scans at increased scan rates, the separation between the anodic and cathodic peak potentials increased and the anodic peak broadened. Although qualitatively reminiscent of the situation with $\mathbf{1}/\mathbf{1}^{2+}$, the distortions from Nernstian behavior were much less (at the same $\nu$) for **2** compared to those of **1**. The voltammetric response of **2** was successfully simulated as an EE mechanism. The wave shapes require that the first et ($\mathbf{2}/\mathbf{2}^{+}$) be *slower* than the second ($\mathbf{2}^{+}/\mathbf{2}^{2+}$) and have a $(1 - \alpha)$ value greater than 0.5. The slow-scan limit of the anodic peak breadth ($\delta E_p = 34$ mV) suggested[36] a value of about +30 mV for $E^{\circ\prime}_1 - E^{\circ\prime}_2$. Excellent fits between experiment and theory were obtained over the scan rate range 1−50 V/s, with representative examples being shown in Figure 10. Average values for the electron-transfer parameters required for the fits are listed in Table 5. The most salient features are $E^{\circ\prime}_1 = -0.775$ V, $k_{s1} = 0.035$ cm s$^{-1}$, $E^{\circ\prime}_2 = -0.762$ V, $k_{s2} >$ 0.2 cm s$^{-1}$ (the fits were insensitive to $k_{s2}$ values greater than 0.2 cm s$^{-1}$). The simulations confirm that $E^{\circ\prime}_2$ is slightly negative of $E^{\circ\prime}_1$ for the $\mathbf{2}/\mathbf{2}^{+}/\mathbf{2}^{2+}$ sequence and that the charge transfer rate of the $\mathbf{2}/\mathbf{2}^{+}$ couple is appreciably below that of the $\mathbf{2}^{+}/\mathbf{2}^{2+}$ couple.

(41) Vollhardt, K. P. C.; Weidman, T. W. *J. Am. Chem. Soc.* **1983**, *105*, 1676.

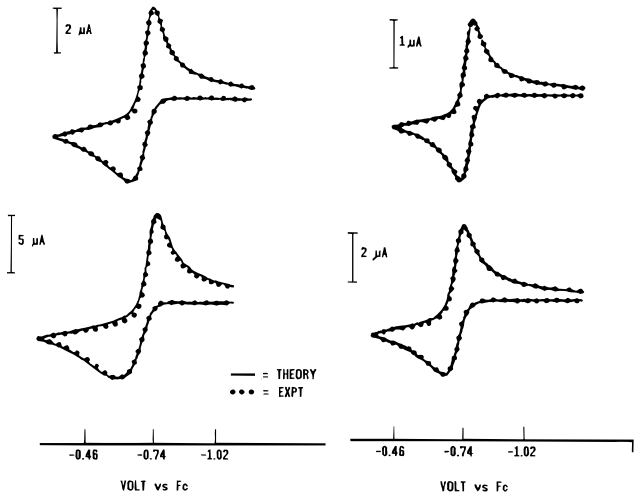


**Figure 10.** CV of 0.71 mM **2** in $CH_2Cl_2$ at Pt, $T = 298$ K. Comparison of experimental data (circles) with simulations (solid lines) at the following scan rates: 1V/s (upper right); 5 V/s (lower right); 10 V/s (upper left); 50 V/s (lower left). Simulation parameters in Table 5.

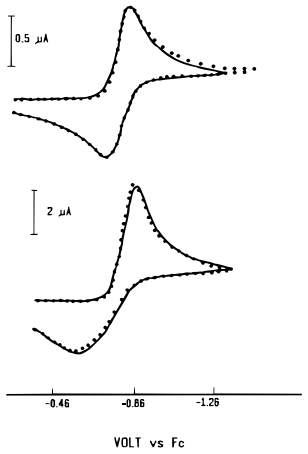


**Figure 11.** CV of 0.43 mM $[\mathbf{2}][PF_6]_2$ in $CH_2Cl_2$, $T = 298$ K. Comparison of experimental data (dots) with simulations (solid lines) at (top) $\nu = 1$ V/s and (bottom) $\nu = 50$ V/s. Simulation parameters in Table 5.

Isolation of the two-electron oxidation product of **2**, namely $\mathbf{2}^{2+}$, provided a rare opportunity to quantify a quasi-reversible multielectron redox process from the point of view of both the reduced and oxidized forms. Thus, CV scans of $\mathbf{2}^{2+}$ gave a close to Nernstian response at slow sweep rates ($E^{\circ\prime}_{\mathrm{app}} = -0.75$ V, $\Delta E_p = 43$ mV, $\delta E_p = 34$ mV at $\nu = 0.05$ V/s) consistent with an EE mechanism in which the *second* et ($\mathbf{2}/\mathbf{2}^{+}$ in this case) is slower than the first ($\mathbf{2}^{2+}/\mathbf{2}^{+}$) and about 35 mV more positive.

At higher $\nu$, deviations from Nernstian behavior were observed and quantatively accounted for by theoretical simulations. Somewhat higher sweep rates were required to view peak asymmetries in $\mathbf{2}^{2+}$ *vs* **2**, as seen in comparing CV scans at $\nu = 1$ V/s in Figures 10 and 11. This observation arises from the relative ordering of the slower and faster et steps in the two redox forms. Since the second et in the reduction of $\mathbf{2}^{2+}$ is the slower one, the rate of the reduction profits by the fact that the scan potential is already *negative* of $\mathbf{2}^{+}/\mathbf{2}$ when the concentration of the monocation becomes dominant, thereby providing overpotential to drive the overall et process. A similar situation does not exist for the oxidation of **2** since the slow step ($\mathbf{2}/\mathbf{2}^{+}$) is the *initial* et reaction. The simulation parameters for fitting the reduction wave of $\mathbf{2}^{2+}$ (Table 5) are in excellent agreement with those found for the same couples in the oxidation of **2**.

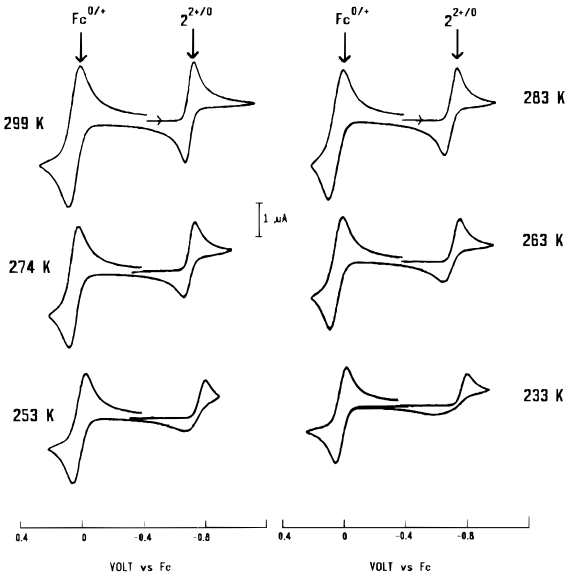


**Figure 12.** CV scans of mixture of 0.43 mM [**2**][$PF_6$]$_2$ and 1.07 mM ferrocene in $CH_2Cl_2$ at various temperatures, $\nu = 0.2$ V/s.

The temperature dependence of the reduction voltammetry of $\mathbf{2}^{2+}$ was briefly investigated to see if other voltammetric features (such as new peaks) might be observed, indicating inadequacy of the EE mechanistic model. No such features were observed. Rather, the $\Delta E_p$ values and degree of peak broadening increased dramatically at lower temperatures. Figure 12 shows these changes compared to that of ferrocene, added as a control to assure that ohmic effects were unimportant. With a scan rate of 0.2 V/s, $\Delta E_p$ for $\mathbf{2}^{2+}$ increased from 50 mV at 298 K (theory for Nernstian $2e^-$ wave: 30 mV) to 135 mV at 253 K (theory: 25 mV). The effect of lowering $T$ on the CV response at a single $\nu$ thus mimics the effect of increasing $\nu$ at a single $T$, both in terms of peak shapes and peak positions, affirming the quasi-reversible EE model of the couple $\mathbf{2}^{2+}$/**2**.

## Discussion

The redox behavior of **1** and **2** is discussed below in terms of mechanism, thermodynamics, and kinetics.

**D.I. Mechanism.** Voltammetric, spectroscopic, and crystallographic data firmly establish that oxidation of both **1** and **2** produces dications having a Rh−Rh bond that is absent in the neutral complexes. This process appears to take place by an EE mechanism, i.e., by successive steps in which the electron transfer and structural reorganization are concomitant. We find no evidence suggesting separation of the et and reorganization processes such as would be required for ECE- or related-type mechanisms. This finding contrasts with those explaining the redox behavior of two other dinuclear systems, namely $[FvMo_2(CO)_6]^{0/2-}$ (eq 4)[19] and $[(\mu\text{-}C_5H_4PPh_2)_2Rh_2(CO)_2]^{0/2+}$ (eq 11).[42] The bridged dinuclear complex **7** oxidizes through a

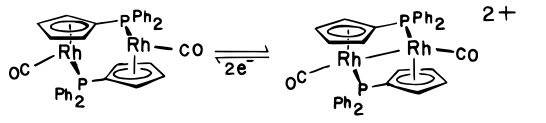


(11)

**7** $\mathbf{7}^{2+}$

chemically reversible but electrochemically irreversible two-electron process to the dication $\mathbf{7}^{2+}$. Under experimentally difficult conditions ($CH_2Cl_2$, $\nu = 10^2-10^3$ V $s^{-1}$), new voltammetric features were attributed to a short-lived intermediate and led to a mechanistic assignment of an ECE process at short observation times.[42] The earlier report concerning $[FvM_2(CO)_6]^{0/2-}$ (M = Cr, Mo, W) assumed an ECE process for the reduction reaction and an EE process for the oxidation (reverse) reaction, but a detailed mechanistic treatment was not reported.[19]

In the present case, the voltammetric curves are completely explained by an EE model for scan rates from 0.05 to 50 V/s. Data are even higher $\nu$ were qualitatively consistent with this model although no quantitative modeling was attempted. If undetected et structural isomers (as found, e.g., in "square schemes")[43] exist for any of the various redox stages of **1** or **2**, they must have lifetimes below a few milliseconds. In the absence of evidence of intermediates, it is appropriate to treat the et and structural changes as being concomitant, thereby facilitating evaluation of the kinetic barriers to electron transfer in terms of molecular reorganization energies.[44]

Inferences may be made about the comparative structures in the electron-transfer sequence by consideration of the relative $k_s$ and $\alpha$ values of the reactions. For both **1** and **2** the 0/1+ reaction is slower than the 1+/2+ reaction, implying that the major structural change occurs as the molecules go between the neutral and monocationic stages. The transfer coefficients are also consistent with this statement. The fact that $(1 - \alpha)$ exceeds 0.5 for these couples (0.66 for $\mathbf{1}/\mathbf{1}^+$, 0.75 for $\mathbf{2}/\mathbf{2}^+$) suggests that the transition state structure for the 0/1+ couple is closer to that of the (product) monocation than that of the (reactant) neutral complex.[45]

**D.II. Kinetics of Electron-Transfer Reactions.** We now identify the nature of structural reorganizations that are likely to accompany et and attempt estimates of their energies. The activation barrier $\Delta G^{\ddagger}$ is the sum of the inner-sphere and outer-sphere contributions, $\Delta G^{\ddagger}_{IS}$ and $\Delta G^{\ddagger}_{OS}$, respectively (eq 12), and the former is related to the inner-sphere reorganizational energy $\lambda_{in}$ by eq 13:

$$\Delta G^{\ddagger} = \Delta G^{\ddagger}_{IS} + \Delta G^{\ddagger}_{OS} \tag{12}$$

$$\Delta G^{\ddagger}_{IS} = \lambda_{in}/4 \tag{13}$$

The value of $\Delta G^{\ddagger}_{OS}$, which arises from solvent reorganization, is readily estimated as ca. 5 kcal $mol^{-1}$ from studies of et kinetics in nonaqueous solvents of metal-$\pi$ complexes of similar charge and size.[46]

Two molecular motions appear likely to contribute to $\lambda_{in}$: rotation around the C−C bond of the fulvalenediyl ligand (**10**) and/or changes in the Rh−Rh distance (**11**). The activation

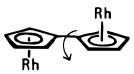


**10**

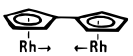


**11**

barrier for rotation has been calculated (EHMO method) as 5.6 kcal $mol^{-1}$ for **1**.[47] In order to estimate the et barrier coupled to motion **11**, we require a value for the Rh−Rh bond enthalpy. The metal−metal bond length in $\mathbf{2}^{2+}$ is 2.83 Å, some 0.14 Å longer than that found in rhodium metal. The bond dissociation

(42) Tommasino, J.-B.; de Montauzon, D.; He, X.; Maisonnat, A.; Poilblanc, R.; Verpeaux, J.-N.; Amatore, C. *Organometallics* **1992**, *11*, 4150.
(43) Evans, D. H.; O-Connell, K. M. In *Electroanalytical Chemistry*; Bard, A. J., Ed.; Marcel Dekker: New York, 1986; Vol. 14, p 113.
(44) Marcus, R. A. *J. Chem. Phys.* **1965**, *43*, 679.
(45) Bard, A. J.; Faulkner, L. R. *Electrochemical Methods*; John Wiley: New York, 1980; p 97.
(46) Weaver, M. J.; Gennett, T. *Chem. Phys. Lett.* **1985**, *113*, 213.
(47) Lichtenberger, D. L.; Gruhn, N. E.; Rempe, M. E.; Geiger, W. E.; Chin, T. T. *Inorg. Chim. Acta* **1995**, *240*, 623.

energy of $Rh_2$ has been reported as 33 kcal mol$^{-1}$ on the basis of gas-phase measurements.[48,49] If one assumes a relationship between bond distance and bond enthalpy such as proposed by Connor,[50] a Rh−Rh bond enthalpy of ca. 25 kcal mol$^{-1}$ is calculated for $\mathbf{2}^{2+}$.

An independent estimate of Rh−Rh bond enthalpy may be obtained from the recent observation that bond distances and Rh−Rh force constants ($F$) are related by $d(Rh_2) = 2.78 - 0.29 \ln F$, where $d(Rh_2)$ is the Rh−Rh bond distance in Å.[49] If a linear relationship is assumed between $F$ and bond enthalpy,[51] a value of 21 kcal mol$^{-1}$ is calculated for $d(Rh_2) = 2.83$ Å, as found in $\mathbf{2}^{2+}$. We employ the average of the two estimates, namely 23 kcal mol$^{-1}$, in our treatment. Since Saveant has shown that $\lambda_{in}$ = bond dissociation energy for dissociative et reactions,[18a] and taking into account eq 13, making and breaking of the Rh−Rh bond in our two systems is thus expected to contribute ca. 6 kcal mol$^{-1}$ to the activation barrier.

The largest activation barrier observed for any one step in the overall two-electron oxidations of **1** and **2** is 7.9 kcal mol$^{-1}$ (Table 5), much lower than the value (ca. 11 kcal mol$^{-1}$) predicted for making and breaking of a Rh−Rh bond coupled to an et process ($\Delta G^{\ddagger} = \Delta G^{\ddagger}_{OS} + \Delta G^{\ddagger}_{IS} = 5 + 6$ kcal mol$^{-1}$). The charge transfer kinetics are inconsistent, therefore, with *full* making and breaking of a Rh−Rh bond in any *one* et step of either $\mathbf{1}/\mathbf{1}^{2+}$ or $\mathbf{2}/\mathbf{2}^{2+}$.

Focusing on the oxidation of **1**, the rather even distribution of activation energies (7.9 kcal/mol for $\mathbf{1}/\mathbf{1}^{+}$, 7.3 kcal/mol for $\mathbf{1}^{+}/\mathbf{1}^{2+}$) implies that the first electron removal results not only in ring rotation but also partial Rh−Rh bond formation (see **12**). The data are *inconsistent* with a model in which ring

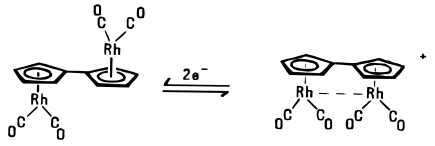


**12**

rotation occurs in the 0/1+ step and metal−metal bond formation occurs separately in the 1+/2+ step, a scenario which would require that the 1+/2+ step be much slower than the 0/1+ step. In fact, the latter is faster than the former.

Turning to **2**, we first note that the sum of the activation barriers of the two et reactions, $\Delta G^{\ddagger}_{tot}$ (eq 14) is ca. 1.2 kcal mol$^{-1}$ *smaller* for $\mathbf{2}/\mathbf{2}^{2+}$ than for $\mathbf{1}/\mathbf{1}^{2+}$ (<14 kcal mol$^{-1}$ *vs* 15.2 kcal mol$^{-1}$, Table 5). Since this is approximately the amount

$$\Delta G^{\ddagger}_{tot} = \Delta G^{\ddagger}_{0/1+} + \Delta G^{\ddagger}_{1+/2+} \qquad (14)$$

of energy required for fulvalenediyl ring rotation, the slightly lower overall activation barrier for $\mathbf{2}/\mathbf{2}^{2+}$ compared to that of $\mathbf{1}/\mathbf{1}^{2+}$ is consistent with the structural differences in the two model systems.

That the first oxidation of **2** is considerably slower than the second suggests that the greater part of the structural change in going from **2** to $\mathbf{2}^{2+}$ occurs in the first et step. Since the $\Delta G^{\ddagger}$ value for this step (7.9 kcal mol$^{-1}$) is still too low to be consistent with full Rh−Rh bond formation in the monocation, it is likely that some tightening of the metal−metal bond is left to the second et reaction, i.e. $\mathbf{2}^{+}$ to $\mathbf{2}^{2+}$.

In summary, the electron-transfer barriers are consistent with an EE mechanistic model, since the measured values of $\Delta G^{\ddagger}_{tot}$ (14−15 kcal mol$^{-1}$) are close to those estimated for two stepwise et reactions involving making and breaking of a Rh−Rh bond (estimate: 16−17 kcal mol$^{-1}$). In the stepwise double oxidation of both **1** and **2**, the first et step is slower than the second, implying that the major structure change accompanies the first electron loss in both systems. For the thermodynamically-unstable intermediate, $\mathbf{1}^{+}$, a structure with a partial Rh−Rh bond is proposed; the structure of $\mathbf{2}^{+}$ may be quite similar.

**D.III. Thermodynamics of Electron-Transfer Reactions.** Both two-electron couples have second-oxidation processes that are thermodynamically facile compared to the first, i.e., $\Delta E°$ is negative. The value of $\Delta E°'$ is so small (−0.02 V) for $\mathbf{2}/\mathbf{2}^{2+}$, however, that it can be stated that the 0/1+ and 1+/2+ potentials are virtually the same for the dppm-bridged complex. By comparison, $\Delta E°$ for $\mathbf{1}/\mathbf{1}^{2+}$ (−0.14 V) is larger in the absolute sense (more negative) by ca. 0.12 V. This implies that the structural change in going from **1** to $\mathbf{1}^{2+}$ stabilizes the *di*cation by ca. 3 kcal/mol compared to the structural change occuring in **2** to $\mathbf{2}^{2+}$. This is consistent with the need for ring rotation in **1**, but not in **2**.

**D.IV. Summary.** In comparing the two-electron oxidations of **1** and **2** we find the following: (1) Both systems require metal−metal bond formation and fracture in the overall two-electron processes. (2) In both cases the electron-transfer rate of the 0/1+ step is slower than that of the 1+/2+ step, suggesting that the major structural change occurs in the former, most likely involving partial metal−metal bond formation. (3) Greater stabilization (by ca. 3 kcal/mol) of the 1+/2+ couple compared to the 0/1+ couple occurs when the overall redox process is accompanied by fulvalenediyl ring rotation. In other words, the one-electron intermediate is comparatively destabilized when its formation requires ring rotation. (4) The net effect of fulvalenediyl ring rotation on single two-electron redox processes is to retard the electron-transfer kinetics of the step involving M−M bond formation and to destabilize the one-electron intermediate, thereby enhancing the thermodynamic driving force for the overall two-electron transfer.

**Acknowledgment.** The authors gratefully acknowledge the financial support of the National Science Foundation (CHE 91-16332 and 94-16611). We also thank Johnson Matthey Co. for a loan of rhodium trichloride. We also thank T. E. Bitterwolf for initial samples of **1** and **2**.

**Supporting Information Available:** Atomic coordinates and thermal parameters for the crystal structure determination of **2** and $[\mathbf{2}][PF_6]_2$ (19 pages). Ordering information is given on any current masthead page.

JA960259A

(48) (a) Gingerich, K. A.; Gupta, S. K. *J. Chem. Phys.* **1978**, *69*, 505. (b) Goursot, A.; Papai, I.; Salahub, D. R. *J. Am. Chem. Soc.* **1992**, *114*, 7452.

(49) Harvey, P. D.; Shafiq, F.; Eisenberg, R. *Inorg. Chem.* **1994**, *33*, 3424.

(50) Connor, J. A. In *Transition Metal Clusters*; Johnson, B. F. G., Ed.; Wiley: Chichester, 1980; p 356 ff.

(51) From the Pauling−Badger relation, see: Sims, L. B.; Lewis, D. E. In *Isotopes in Organic Chemistry*; Buncel, E., Lee, C. C., Eds.; Elsevier: Amsterdam, 1984; Vol. 6, p 184 ff.